

Fragmentation of ${}^4\text{He}$, ${}^{12}\text{C}$, ${}^{14}\text{N}$, and ${}^{16}\text{O}$ nuclei in nuclear emulsion at 2.1 GeV/nucleon

H. H. Heckman, D. E. Greiner, P. J. Lindstrom, and H. Shwe

Lawrence Berkeley Laboratory and Space Sciences Laboratory, University of California, Berkeley, California 94720

(Received 29 August 1977)

A comparative study of the fragmentation of ${}^4\text{He}$, ${}^{12}\text{C}$, ${}^{14}\text{N}$, and ${}^{16}\text{O}$ nuclei, $E = 2.1$ GeV/nucleon, has been made by using nuclear emulsion detectors. The interaction mean-free paths (cm) for these nuclei in emulsion are 21.8 ± 0.7 , 13.8 ± 0.5 , 13.1 ± 0.5 , and 13.0 ± 0.5 , respectively. These data are discussed in terms of optical models and geometrical theories. Fragmentation reactions initiated by ${}^{12}\text{C}$, ${}^{14}\text{N}$, and ${}^{16}\text{O}$ projectiles that exhibit no target excitation, i.e., that possess no low energy particle emission, are selected for special study of projectile fragmentation. The projected angular distributions of $Z = 1$ and 2 secondaries from these interactions are reported, as are the prong-number and charge-multiplicity distributions. The angular distributions are independent of the projectile and exhibit features of limiting fragmentation.

NUCLEAR REACTIONS Emulsion exp., ${}^4\text{He}$, ${}^{12}\text{C}$, ${}^{14}\text{N}$, and ${}^{16}\text{O}$ at 2.1 GeV/A; measured mean-free-path lengths; projectile fragmentation reactions; angular, number, and charge multiplicity distributions. Optical and geometrical models; limiting fragmentation.

I. INTRODUCTION

With the discovery of heavy nuclei in primary cosmic rays in 1948,¹ studies of the nucleus-nucleus interaction at high energies became possible. Early work was concerned with interaction mean-free paths and the production of fragments, as these data were most pertinent to the physics of cosmic rays.² Although encumbered by the low intensities and uncertainties in charge and energy determination of the heavy nuclei, later cosmic-ray experiments have revealed many of the general features of the nucleus-nucleus interaction, e.g., production of shower particles, α -particle production from both target and projectile nuclei, production of heavy nuclei.³⁻⁹ In these experiments, as in the present one, the nuclear research emulsion was used as the target and detector.

In this paper we present experimental results on the interactions in nuclear research emulsions of ${}^4\text{He}$, ${}^{12}\text{C}$, ${}^{14}\text{N}$, and ${}^{16}\text{O}$ nuclei accelerated in 2.1 GeV/nucleon at the Bevatron. The interaction mean-free paths measured for these ions are compared with optical-model calculations, and are also presented in terms of a two-parameter expression for the geometrical cross section (Sec. III A). These parameters are r_0 , the constant of proportionality defined by the expression for the nuclear radius $r_i = r_0 A_i^{1/3}$, and b , the overlap parameter. The quantity b is equal to $\Delta r / r_0$, where Δr is the geometrical overlap between the colliding nuclei. In this experiment we find that about 12% of the interactions of ${}^{12}\text{C}$, ${}^{14}\text{N}$, and ${}^{16}\text{O}$ beam particles with emulsion nuclei lead to "pure" projectile frag-

mentation, characterized by no detectable target fragmentation, i.e., no low-energy, charged-particle emission in the interaction. We have selected these interactions for specific study of the projected angular distribution for charge $Z = 1$ and 2 secondary fragments (See. III B) and of the topological features of the fragmentation of ${}^{12}\text{C}$, ${}^{14}\text{N}$, and ${}^{16}\text{O}$ nuclei, presented in terms of the prong-number and charge-multiplicity distributions (Sec. III C).

An interesting aspect of this experiment is the possibility for interpreting the angular distribution measurements in terms of the hypothesis of limiting fragmentation.¹⁰ Because of the large separation in rapidity ($y = \tanh^{-1}\beta_L$) between the projectile and target fragments at relativistic energies, limiting fragmentation dictates that no correlations exist between the projectile and target fragments. Bevatron experiments on the 0° fragmentation of relativistic heavy-ion projectiles at $E = 1.05$ and 2.1 GeV/nucleon have shown that the modes of fragmentation are independent of the mass of the target nucleus,¹¹⁻¹³ a result that is compatible with the principle of limiting fragmentation. Consequently, the fragmentation cross sections for the reaction $B + T \rightarrow F + \dots$ can be factored according to $\sigma_{BT}^F = \gamma_B^F \gamma_T$ where γ_B^F is a function of the beam B and fragment F nuclei; and γ_T , the target factor, is a function of target T . Exceptions of strict factorization have been observed for fragmentation reactions in hydrogen (where γ_T exhibits a weak dependence on the mass of fragment F),¹³ in helium,¹⁴ and for heavy targets where single-nucleon stripping is enhanced by the Coulomb dissociation of ${}^{12}\text{C}$ and ${}^{16}\text{O}$ projectiles in the virtual

photon field of the target nucleus.^{13,15} By selecting interactions in emulsion with no visible target fragmentation, we have defined a subset of interactions where the nature of the reaction is specified in the low-rapidity region. Thus a comparison of the angular distribution of the high-rapidity projectile fragments measured in this experiment with the results of the single-particle inclusive experiments of Greiner *et al.*,¹⁶ where there were no restrictions on the fragmentation of the target, provides for a more stringent test of the limiting fragmentation hypothesis.

II. PROCEDURE

The emulsion stacks used in this experiment were fabricated from Ilford G.5 pellicles, 600 μm thick. The stacks were exposed to beams of 2.1-GeV/nucleon ^4He , ^{12}C , ^{14}N , and ^{16}O nuclei parallel to the emulsion planes. The scanning technique for each beam was to select an incident ion 1 to 2 mm from the entrance edge and scan along the track until the ion interacted or left the pellicle. The beginning and terminal points of each track segment were recorded by three-coordinate digitized microscopes with 1- μm readout accuracy. Recorded for each interaction were beam type, the event number, the emulsion plate number and grid coordinate (a 1-mm grid system was photographed on the emulsion glass interface of each pellicle), the number, and, for relativistic secondaries, the charges of the secondary fragments. The interactions were qualitatively classified as to type, depending upon their visual characteristics:

Type (1): Projectile fragmentation only. No visible target fragmentation. Also denoted as $n_h = 0$ events, where n_h is the number of nonrelativistic particles emitted from the interaction.

Type (2): Projectile fragmentation with target breakup, $n_h \geq 1$.

Type (3): Catastrophic destruction of projectile and target nuclei. No forward-cone fragments from the projectile are evident.

Type (4): Target fragmentation only. No detectable change in charge of projectiles, i.e., the inverse of type (1).

We have selected events of type (1) for special examination in that they represent the "cleanest" examples of projectile fragmentation. These events were intensively examined for all secondary fragments. Because the velocities of nuclear fragments of the beam projectile are near the velocity of the beam, $\beta = 0.95$, the grain densities of the secondary tracks are related to Z^2 of the fragment. Charge estimates for ionizing tracks $Z \leq 3$ were thus greatly simplified, requiring only rud-

imentary grain-density measurements. All secondary tracks with $Z \geq 4$ were grouped together, and no systematic attempt was made to resolve these higher charges. However, although not fundamental to the analysis of the data, charge estimates of all tracks were made by the scanner-measurer by inspecting the relative ionization rates of the incident beam and secondary particles.

The spatial configuration of each event was reconstructed by measuring a pair of x, y, z coordinates separated by at least 500 μm , on each of the primary and secondary tracks. These coordinate data were digitally recorded on magnetic tape accompanied by pertinent indicative information. The projected angular resolutions between two track segments attained in these measurements were $\pm 0.16^\circ$ [standard deviation (SD)] in the horizontal plane and $\pm 0.39^\circ$ in the vertical plane.

III. RESULTS AND DISCUSSION

A. Interaction mean-free-path lengths

The path length followed for each species of beam was sufficient to obtain at least 10^3 interactions. Table I presents a breakdown of these interactions into the numbers observed for types (1)–(4), N_1 through N_4 , and their sum N_{obs} . An analysis of the data obtained from the original scanning led us to conclude that the scanning efficiency was near 100% for events in which the difference between the charges of the beam and principal fragment is $\Delta Z = Z_B - Z_F \geq 2$. However, events for which $\Delta Z = 0$ or 1, e.g., when the projectile undergoes neutron or proton stripping, tend to be missed. Of particular concern are those fragmentation events that exhibit little or no evidence for excitation of the target nucleus. Clearly, events of type (1) in which the projectile undergoes neutron loss are undetectable in the emulsion. Also, type (1) events that involve the loss of a single charge by the projectile, where the resulting fragment proceeds with no noticeable change in direction (whether or not it is accompanied by a minimally ionizing $Z = 1$ particle), become progressively more difficult to detect as the charge of the projectile increases. These conjectures were confirmed upon rescanning about one-third of the ^{12}C , ^{14}N , and ^{16}O track data. Out of 1059 events, the rescanning contributed 16 new events, all of which were types (1) or (4), having $\Delta Z = 0, 1$ only. No new type (2) or (3) events were detected.

To correct N_{obs} for these scanning biases we have used the isotope production cross sections of Lindstrom *et al.*^{13,17} to compute the probabilities for $\Delta Z = 0$ and 1 fragmentation events for ^{12}C and ^{16}O ions in emulsion at 2.1 GeV/nucleon.

TABLE I. Interaction mean-free-path length data. Tabulated are N_i , the number of observed interactions of type (i), $N_{\text{obs}} = \sum_i N_i$, $N_{\text{total}} = N_{\text{obs}}$ corrected for scanning losses of $\Delta Z = 0$ and 1 events, and $N_{\Delta Z \geq 1}$, the number of charge-changing ($\Delta Z \geq 1$ events). The interaction lengths evaluated from N_{total} and $N_{\Delta Z \geq 1}$ are λ_{total} and $\lambda_{\Delta Z \geq 1}$, respectively.

| Measurements | ${}^4\text{He}$ | ${}^{12}\text{C}$ | Beam ${}^{14}\text{N}$ | ${}^{16}\text{O}$ |
|----------------------------------|-----------------|-------------------|---------------------------|-------------------|
| N_1 | 104 | 149 | 123 | 119 |
| N_2 | 500 | 533 | 506 | 600 |
| N_3 | 353 | 325 | 376 | 249 |
| N_4 | 54 | 88 | 54 | 55 |
| N_{obs} | 1 011 | 1 095 | 1 059 | 1 023 |
| N_{total} | 1 011 | 1 111 \pm 39 | 1 090 \pm 47 | 1 092 \pm 38 |
| $N_{\Delta Z \geq 1}$ | 957 | 1 044 \pm 39 | 1 031 \pm 45 | 1 040 \pm 36 |
| Path length (cm) | 22 080 | 15 302 | 14 895 | 14 174 |
| λ_{total} (cm) | 21.8 \pm 0.5 | 13.8 \pm 0.5 | 13.7 \pm 0.6 | 13.0 \pm 0.5 |
| $\lambda_{\Delta Z \geq 1}$ (cm) | 23.1 \pm 0.8 | 14.7 \pm 0.6 | 14.5 \pm 0.6 | 13.6 \pm 0.5 |

These probabilities are 16.1% and 16.4%, respectively. The final corrections to N_{obs} are summarized in Table II. The largest correction for missed $\Delta Z = 0, 1$ events is for ${}^{16}\text{O}$, where 39% (or about 4% of N_{total}) of these types of events are undetected. Owing to improved detection efficiency for these events as Z decreases, this fraction decreases to 1% for ${}^{12}\text{C}$, indicating that the loss of $\Delta Z = 0, 1$ events for ${}^4\text{He}$ beams is also small. We have, therefore, made no corrections to the ${}^4\text{He}$ data.

Listed in Table I are the numbers of events, $N_{\Delta Z \geq 1}$, for which the charge of the principal fragment differs from that of the incident ion by $\Delta Z \geq 1$. The mean-free path derived can then be directly compared with experiments that rely on the differences in dE/dx , hence charge, between the incident and fragment nuclei to signify an interaction.¹⁸ Table I concludes with the measured interaction mean-free paths, λ_{total} (cm) and $\lambda_{\Delta Z \geq 1}$ (cm) in nuclear emulsion for ${}^4\text{He}$, ${}^{12}\text{C}$, ${}^{14}\text{N}$, and ${}^{16}\text{O}$ nuclei, $E = 2.1$ GeV/nucleon.

The C, N, and O data confirm, within the accuracies of the cosmic-ray experiments, the mean values of the interaction mean-free paths

TABLE II. Corrections to N_{obs} for undetected $\Delta Z = 0$ and 1 events.

| $N_{\Delta Z=0,1}$ | ${}^{12}\text{C}$ | Beam ${}^{14}\text{N}$ | ${}^{16}\text{O}$ |
|--------------------------------|-------------------|---------------------------|-------------------|
| Observed | 163 \pm 17 | 146 \pm 28 | 110 \pm 12 |
| Expected ^a | 179 \pm 18 | 177 \pm 17 ^b | 179 \pm 17 |
| Correction to N_{obs} | 16 \pm 25 | 31 \pm 33 | 69 \pm 21 |

^a Expected number of $N_{\Delta Z=0,1}$ events were computed by using the cross sections given in Refs. 13 and 17.

^b Evaluated with the average of the ${}^{12}\text{C}$ and ${}^{16}\text{O}$ fragmentation cross sections.

for cosmic-ray M nuclei ($6 \leq Z \leq 9$) in emulsion as summarized by Cleghorn¹⁹ and Waddington.²⁰ The average of all measurements of $\lambda(M)$ cited in Refs. 19 and 20 gives an energy-independent interaction mean-free path of 13.3 ± 0.6 cm. Recent measurements of the mean-free path of Bevatron-accelerated 2.0 GeV/nucleon ${}^{16}\text{O}$ ions in emulsion have been made by Jakobsson *et al.*²¹ (13.7 ± 1.1 cm) and Judek²² (12.6 ± 0.5 cm). Our measured value of $\lambda(\text{He}) = 21.8 \pm 0.7$ cm is $15 \pm 5\%$ greater than the average value of $\lambda(\text{He}) = 18.9 \pm 0.8$ cm evaluated from the summary given by Lohrmann and Teucher²³ for the interactions of cosmic-ray primary and secondary α particles (the latter from the fragmentation of heavy nuclei) in emulsion at kinetic energies $E > 6$ GeV/nucleon. Neither the cosmic-ray results nor the individual contributions from our five scanners to our α data showed any significant anomalies that could account for the differences between the respective values of $\lambda(\text{He})$. In view of possible differences in scanning and selection criteria, uncertainties in the identification of cosmic-ray α nuclei, and the provocative evidences that the interaction path lengths of light secondary nuclei exhibit anomalously short mean-free paths,^{19,22} a resolution of this difference must await further experimental inquiry.

An empirical expression for the interaction cross section that traditionally has been used to interpret the data given in Table I is the geometrical formula first proposed by Bradt and Peters,²⁴

$$\sigma_{BT} = \pi r_0^2 (A_B^{1/3} + A_T^{1/3} - b)^2, \quad (1)$$

where A_B and A_T are the mass numbers of the beam and target nuclei, respectively; b is the overlap parameter, and r_0 is the constant of proportionality in the expression for the geometrical

nuclear radius $r_i = r_0 A_i^{1/3}$. Consistent fits to heavy-ion reaction cross-section data have been reported for r_0 and b in the ranges $1.15 \leq r_0 \leq 1.45$ fm and $0 \leq b \leq 1.5$,^{19,24,25} owing to the fact that the parameters r_0 and b are coupled. This is exemplified in the present experiment where, with an assumed constant overlap parameter b for all elements in emulsion, the mean-free path data can be fitted, by using Eq. (1), to confidence levels $<25\%$ ($\chi^2 \leq 2.7$ for two degrees of freedom) when r_0 and b are in the range $1.44 \leq r_0 \leq 1.72$ fm and $1.28 \leq b \leq 1.92$. The calculated mean-free-path lengths are given by the expression $\lambda_{\text{calc}} = [\sum_i n_i(T) \sigma_{BT}]^{-1}$, where $n_i(T)$ is the number of target nuclei T per milliliter in emulsion,²⁶ and σ_{BT} is the interaction cross section—taken to be Eq. (1) in this case. However, the transmutation cross sections ($\Delta Z \geq 1$) measured by Lindstrom *et al.*¹⁷ for ^{12}C and ^{16}O , $E = 2.1$ GeV/nucleon, give evidence that the overlap b is not constant but depends upon the mass, i.e., radius, of the beam nucleus. From any geometrical description of nuclei, one can intuitively argue that the b parameter should be dependent on the radii of colliding nuclei. We have found that the theoretical results of Barshay, Dover, and Vary²⁷ and Karol²⁸ are particularly useful in addressing this problem.

In their investigation of the question of the validity of factorization of total cross sections in nucleus-nucleus collisions, Barshay *et al.*²⁷ calculated the total reaction cross sections using a geometrical nuclear model and an impact parameter representation of the scattering amplitude, which can be considered to be the optical limit of the Glauber theory. In the same limit, Karol has derived an analytical approximation for the total nucleus-nucleus reaction cross section²⁸ that gives values in good agreement with those given by Barshay *et al.* Karol's "soft-spheres model" utilizes the experimentally measured density-distribution parameters (i.e., the half-central-density radius and the 90%–10% surface-skin-thickness parameter) and energy-dependent nucleon-nucleon cross sections.

To fit the measured mean-free-path data to the optical model, we employ Karol's analytical expression for the reaction cross section σ_{BT} , taking the average nucleon-nucleon cross section $\bar{\sigma}$ to be given by $K\bar{\sigma}(2.1)$ where $\bar{\sigma}(2.1)$ is the average nucleon-nucleon cross section at 2.1 GeV, and K is an adjustable parameter. The best fit to the experimental data is obtained when $K = 0.52 \pm 0.06$, which corresponds to effective proton-proton (neutron-neutron) and proton-neutron inelastic cross sections of 23.1 ± 1.3 and 22.2 ± 1.3 mb, respectively.

Using the effective nucleon-nucleon cross sec-

tion $\bar{\sigma}$ thus determined, we now examine the possibility of presenting the calculated reaction cross section of Karol and Barshay *et al.* in the form of the Bradt-Peters relation, Eq. (1). We find that the calculated nucleus-nucleus reaction cross sections do exhibit the form of Eq. (1), to excellent approximation, when the cross sections are ordered to A_{min} , the lighter of the beam and target nuclei. In Fig. 1 we plot $\sigma_{BT}^{1/2}$ versus $A_B^{1/3} + A_T^{1/3}$, where σ_{BT} is computed for a large variety of nuclei, using the effective nucleon-nucleon cross section $\bar{\sigma} = 0.52\bar{\sigma}(2.1)$. The computational results display a family of approximately parallel lines, each identified with a given A_{min} , whose slope is r_0 and intercept with the abscissa is the mass-dependent overlap parameter $b(A_{\text{min}})$. In Figs. 2(a) and 2(b) we present the results of a least-squares fit to a number of sets of computed cross sections, each designated by A_{min} ($\equiv A_B$) with $A_T \geq A_{\text{min}}$, from which we have deduced r_0 and $b(A_{\text{min}})$ as a function of A_{min} . The fits to the calculated cross sections reveal that r_0 , Fig. 2(a) is insensitive to A_{min} , with the systematic variations in r_0 less than the typical statistical error for r_0 . The mean value of r_0 for all A_{min} , $1 < A_{\text{min}} < 60$, is $\bar{r}_0 = 1.36 \pm 0.02$ fm. The overlap parameters $b(A_{\text{min}})$, Fig. 2(b), are all positive, which indicates that a finite

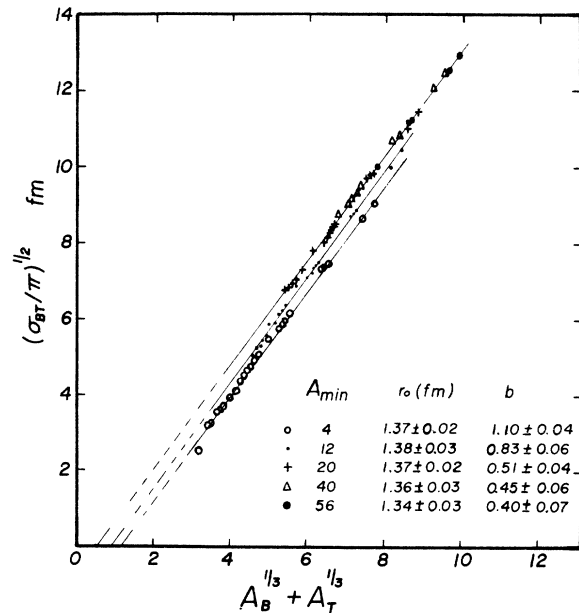


FIG. 1. Reaction cross sections computed from soft-sphere model, Ref. 28, by using nucleon-nucleon cross sections adjusted to fit the emulsion mean-free-path data. Cross sections are ordered by A_{min} , the mass of the lighter of the two interacting nuclei in terms of the Bradt-Peters relation, Eq. (1). Least-squares fits to the computed cross sections are indicated for $A_{\text{min}} = 4, 12, 20, 40,$ and 56 .

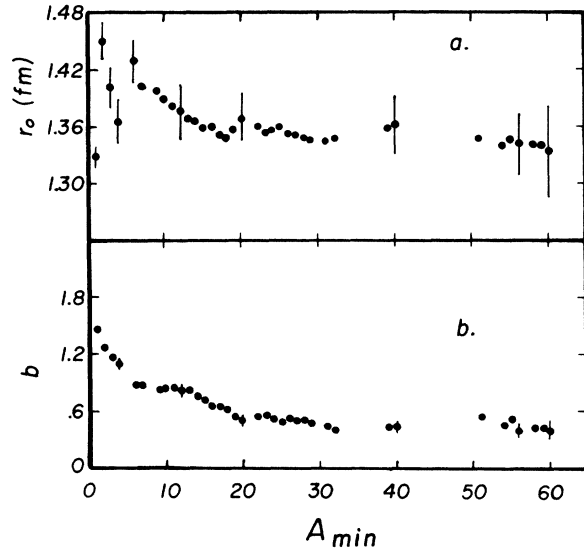


FIG. 2. (a) The radius r_0 and (b) overlap b parameter deduced from the least-squares fits of soft-sphere model calculations versus A_{min} .

overlap of the colliding nuclei, hence, nuclear transparency, is necessary to produce visually detectable reactions in nuclear emulsion. Qualitatively, the overlap parameter is largest for the light nuclei. It decreases approximately linearly until $A_{min} \approx 30$, then becomes constant for $A_{min} \geq 30$. Thus, for heavy nuclei, the cross sections approach those characteristics of the geometric cross section $\sigma = \pi r_0^2 (A_B^{1/3} + A_T^{1/3})^2$.

Vary²⁹ has shown that Glauber (nucleus-nucleus scattering) amplitudes lead to a total nucleus-nucleus reaction cross section that can be expressed in the Bratt-Peters form, given by

$$\sigma = \pi r_0^2 [A_B^{1/3} + A_T^{1/3} - b_0 (A_B^{-1/3} + A_T^{-1/3})]^2 \text{ fm}^2, \quad (2)$$

where $r_0 = 1.36$ fm and $b_0 = 0.75$. In the overlap term $b = b_0 (A_B^{-1/3} + A_T^{-1/3})$, the quantities $A^{-1/3} \propto r^{-1}$ are identified with effects due to the curvature of the nuclear surfaces. Although Vary's expression for b includes contributions from both interacting nuclei, the general feature of b is that its value is dominated by the smaller nuclear

mass, and becomes insensitive to changes in A_B and A_T when they are large, a behavior qualitatively similar to that illustrated in Fig. 2(b).

To relate the mean-free-path data of this experiment to Vary's expression, Eq. (2), we take the following approach: (i) Because of the insensitivity of r_0 to both A_{min} , Fig. 2(a), and the average nucleon-nucleon cross section $\bar{\sigma}(\Delta r_0/r_0 \approx -0.03$ when K increases from 0.4 to 1.0), we assume r_0 is constant, equal to 1.36 fm; and (ii) because changes in $\bar{\sigma}$ are therefore principally contained in the overlap parameter b , we take b_0 as an adjustable parameter in Eq. (2) to fit the mean-free-path lengths, Table I. In Table III we give the results of this analysis, and list the measured and computed mean-free-path lengths using the cross sections σ_{BT} evaluated with the fitted parameters $K = 0.52$ in the soft-sphere model and $b_0 = 1.11$ in Eq. (2).

Finally, having determined the parameters K and b_0 from our measured path lengths in emulsion, we are able to compare directly the nucleus-nucleus cross sections implied by the emulsion data with those measured by Lindstrom *et al.*¹⁷ for several target nuclei. This is done in Table IV.

Thus we find that by using as adjustable parameters the average nucleon-nucleon cross section $\bar{\sigma}$ in the soft-sphere model and b_0 in Vary's expression, the mean-free-path theories of ${}^4\text{He}$, ${}^{12}\text{C}$, ${}^{14}\text{N}$, and ${}^{16}\text{O}$ can be well accounted for by the respective theories. However, the one parameter approach we have taken to fit the emulsion data clearly fails for hydrogen targets, as indicated in Table IV. Because the emulsion data require an effective nucleon-nucleon cross section that is about 50% of the free nucleon-nucleon cross section at 2.1 GeV, we are led to the conclusion that the effective nucleon-nucleon cross section for nucleon removal, i.e., transmutation, in heavy-ion collisions (the only type of reaction detectable in emulsion) is significantly suppressed in nucleus-nucleus collisions. This argument is supported by the agreement between the cross sections deduced from this experiment and those measured by Lindstrom *et al.*,¹⁷ Table IV. The notable disagreement

TABLE III. Interaction mean-free lengths (cm) in Ilford emulsion calculated by using parameters K and b_0 that best fitted experimental data. The composition of Ilford G.5 emulsion used for the calculations is given in Ref. 26.

| Fitted parameters | Beam | | | |
|-------------------|-----------------------|-------------------|-------------------|-------------------|
| | ${}^4\text{He}$ | ${}^{12}\text{C}$ | ${}^{14}\text{N}$ | ${}^{16}\text{O}$ |
| Experiment | 21.8 ± 0.7 | 13.8 ± 0.5 | 13.7 ± 0.6 | 13.0 ± 0.5 |
| Karol (Ref. 28) | $K = 0.52 \pm 0.06$ | 22.5 | 14.1 | 12.4 |
| Vary [Eq. (2)] | $b_0 = 1.11 \pm 0.05$ | 22.2 | 14.2 | 12.5 |

TABLE IV. Comparison of measured cross sections by Lindstrom *et al.* (Ref. 17) with computed cross sections using parameters K and b_0 obtained from the emulsion data. The cross sections are given in mb.

| Beam | Target | | | | |
|---------------------|--------------|---------------|---------------|---------------|---------------|
| ^{12}C | H | C | S | Cu | Pb |
| Lindstrom (exp) | 258 ± 21 | 826 ± 23 | 1250 ± 51 | 1730 ± 36 | 2960 ± 65 |
| Karol ($K=0.52$) | 181 | 788 | 1320 | 1800 | 3190 |
| Vary ($b_0=1.11$) | 167 | 757 | 1250 | 1770 | 3300 |
| ^{16}O | | | | | |
| Lindstrom (exp) | 361 ± 24 | 1022 ± 25 | 1420 ± 51 | 1950 ± 41 | 3270 ± 82 |
| Karol | 230 | 918 | 1500 | 2000 | 3470 |
| Vary | 225 | 877 | 1400 | 1950 | 3540 |

for hydrogen targets implies that, for this case, the effective nucleon-nucleon cross section is within about 10% of the nucleon-nucleon inelastic cross section. The dichotomy between the $\bar{\sigma}_{NN}$'s to account for the nucleon-nucleus and nucleus-nucleus transmutation reactions appears to be real, and one that requires further theoretical and experimental investigation.

We find it provocative that the reaction cross sections given by Karol²⁸ and Barshay *et al.*,²⁷ exhibit the form of the Bradt-Peters relation, albeit modified in that the overlap parameter b is now a function of A_{min} . Although the representation of the theoretical cross sections in such a geometric model may not be entirely valid, the parameters r_0 and b deduced from the optical-model theories are physically realistic.

B. Angular distributions of $Z = 1$ and 2 secondaries from projectile fragmentation

The measurements of single-particle inclusive spectra by Greiner *et al.*¹⁶ have shown that the longitudinal momentum distributions of secondary nuclei produced by the fragmentation of ^{12}C and ^{16}O beam projectiles are typically Gaussian-shaped in the projectile rest frame, and have widths (SD) from about 50 to 200 MeV/ c that depend only on the fragment and beam nuclei. To about 10% accuracy, these characteristics of the momentum distributions are independent of the target. Our present study of projectile fragmentation in nuclear emulsion uses a sample of ($n_h=0$) events in which no low-energy charged particles were produced in the interaction. Because these particular events show no visual evidence of target excitation, they are taken to represent nuclear collisions that occur at large impact parameters.

Figure 3 is an example of a "pure" projectile-fragmentation event in emulsion, typical of the

interactions selected for this investigation. Here, a 2.1-GeV/nucleon ^{14}N nucleus fragments into three $Z=2$ secondaries and one $Z=1$ secondary. Approximately 100 fragmentation events of the type illustrated were observed for each of the ^{12}C , ^{14}N , and ^{16}O beams. Note that the absence of any low-energy target-associated prongs precludes target identification. Under this criterion, most, if not all, hydrogen target events are excluded, because such interactions would be classified as $n_h=1$ events owing to the recoil of the target. In fact, several examples of hydrogen-target-induced fragmentations were kinematically identified.

Figures 4, 5, and 6 present, respectively, the composite projected angular distribution for $Z=1$ and $Z=2$ secondaries from the fragmentation of ^{12}C , ^{14}N , and ^{16}O nuclei at 2.1 GeV/nucleon. The angular distribution data were combined because we observed no statistically significant difference between them, and, based on the results of Greiner *et al.*¹⁶ and Lepore and Riddell,³⁰ we expected none. Because the nuclear fragments of the projectile proceed with velocities nearly equal to that of the incident ion, the secondary nuclei have energies ≈ 2.1 GeV/nucleon, hence ionization-loss rates $\approx Z^2(dE/dx)_{\text{min}}$. The $Z=1$ and $Z=2$ secondary nuclei are thus easily identified by their differences in grain density (see Fig. 3). The composition of $Z=1$ secondaries includes, in fact, all singly-charged particles (p, d, π , etc.) having grain densities $g \leq 1.4 g_{\text{min}}$. Low-velocity $Z=1$ secondaries with grain densities about $4 g_{\text{min}}$ can, in principle, be included in the $Z=2$ data. However, such tracks tend to display large multiple scattering that would affect their elimination from the sample. The $Z=2$ data are therefore predominantly He nuclei.

The projected angular distribution for $Z=1$ particles, Fig. 4, shows a peaked distribution at 0° with respect to the beam direction, with about 99% of all secondaries restricted to the forward hem-

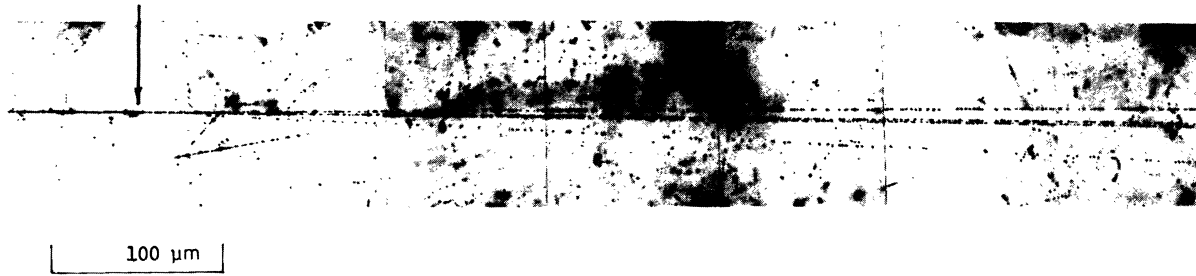


FIG. 3. Photomicrograph of the fragmentation of a 2.1-GeV/ N ${}^{14}\text{N}$ nucleus in nuclear emulsion. The point of interaction is indicated by the arrow. The ${}^{14}\text{N}$ enters from the left, fragments into $3\text{He} + \text{H}$, with no emission of low-energy, heavily ionizing tracks.

isphere. In Fig. 5 we show the structure of the $Z=1$ distribution for $\theta_{\text{proj}} \leq 16^\circ$. The projected angular distribution has a narrow central peak, superimposed upon, and distinct from, a broader distribution. The observed projected angular distribution for $Z=2$ secondaries is given in Fig. 6. This distribution is dominated by a narrow forward peak, having a characteristic width $\leq 1^\circ$. There is evidence for production angles significantly greater than can be associated with the central distribution, although all $Z=2$ secondaries are confined to $\theta_{\text{proj}} < 7^\circ$.

To interpret the $Z=1, 2$ angular distributions (Figs. 5 and 6), we refer to the experiments of Greiner *et al.*¹⁶ and to the work of Lepore and Riddell.³⁰ The latter authors have treated the fragmentation of high-energy nuclei by a quantum mechanical calculation using the sudden approximation and shell-model functions and have shown that (a) the projected momentum distributions in the projectile frame are, to good approximation, Gaussian, with equal standard deviations, and (b) the standard deviation widths of these distributions are to first order given by

$$\sigma = [m_p \omega A_F (A_B - A_F) / 2A_B]^{1/2} \text{ MeV}, \quad (3)$$

where A_B = mass number of beam, A_F = mass number of fragment, m_p = mass of proton, and $\omega = 45A_B^{-1/3} - 25A_B^{-2/3}$.

In Table V we tabulate the average momentum widths σ (SD) for the CNO group, as measured by Greiner *et al.* and evaluated from Eq. (3), and the corresponding angular widths $\sigma(\theta_{\text{proj}})$ for the $Z=1, 2$ isotopes. To intercompare the data in Table V, one must bear in mind that the longitudinal momentum data of Greiner *et al.*¹⁶ are based only on production angles less than 0.72° . Within this acceptance angle the longitudinal momentum spectra for all isotopes were Gaussian shaped (in the projectile frame), with the exception of the spectrum for protons, which was consistently ex-

ponential in shape. For the purposes of Table V, however, we have taken all momentum widths to be $\sigma(\text{SD})$. From the isotopic production cross-section data of Lindstrom *et al.*,¹³ we estimate the production ratios in nuclear emulsion for the hydrogen isotopes to be $p:d:t=1:0.25:0.1$; and for the helium isotopes ${}^4\text{He}:{}^3\text{He}=1:0.31$. Included in Table V are the resultant weighted val-

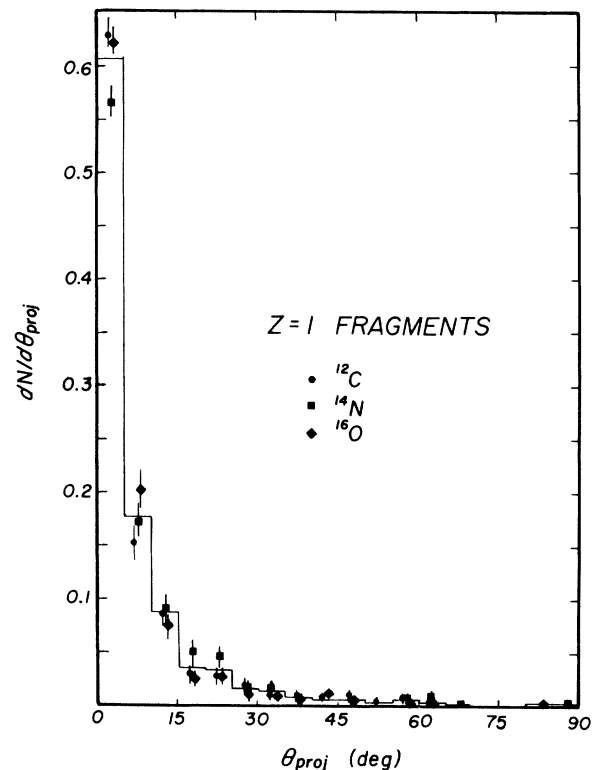


FIG. 4. Projected angular distribution for $Z=1$ fragments, produced in the forward hemisphere by the fragmentation of ${}^{12}\text{C}$, ${}^{14}\text{N}$, and ${}^{16}\text{O}$ projectiles. All interactions are of the $n_h=0$ type, as illustrated in Fig. 3. Beam energy is 2.1 GeV/ N .

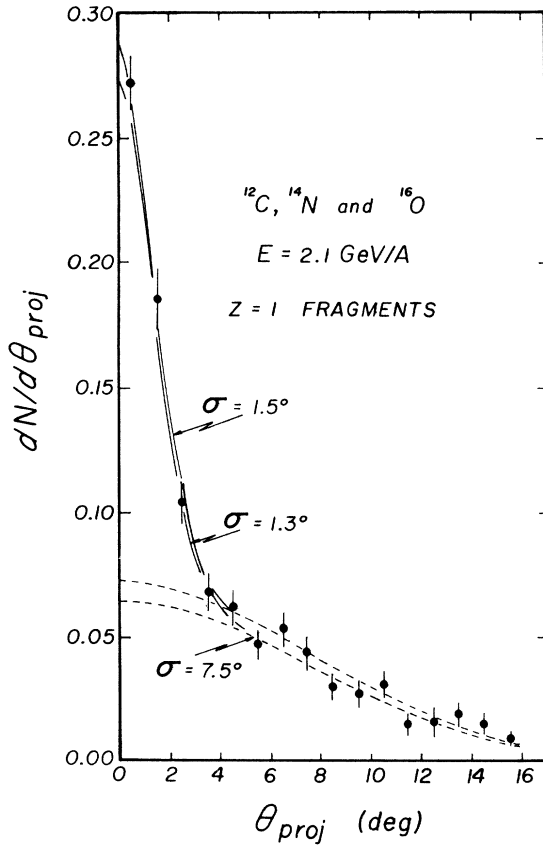


FIG. 5. The combined projected angular distribution for $Z=1$ fragments, C, N, and O projectiles, $\theta_{\text{proj}} \leq 16^\circ$. The curves drawn through the data are the sums of two Gaussian distributions, $\sigma=1.3^\circ$ (1.5°), and 7.5° , normalized to unit areas.

ues of $\sigma(\theta_{\text{proj}})$ for the $Z=1, 2$ isotopes, denoted as $\sigma_{Z=1}$ and $\sigma_{Z=2}$, which are the standard deviations of the projected angular distribution of $Z=1$ and 2 secondary nuclei produced by the fragmentation of

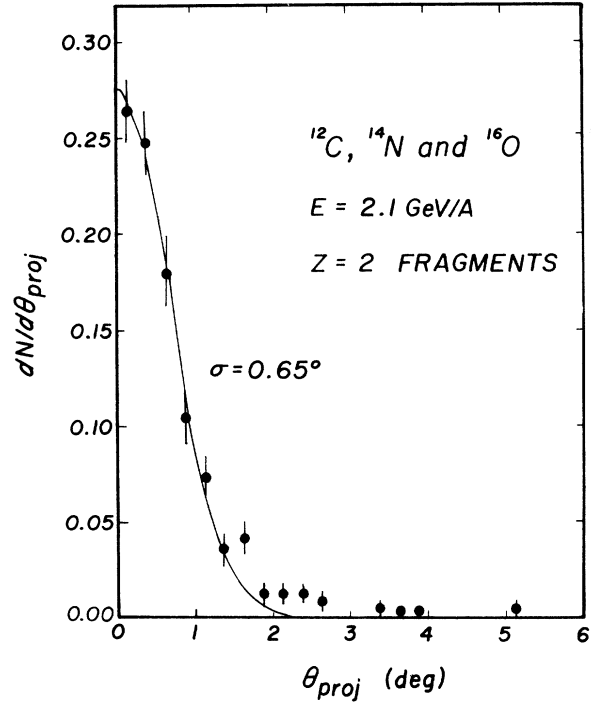


FIG. 6. Angular distribution, projected onto the emulsion plane, for He ($Z=2$) fragments from the fragmentation of ^{12}C , ^{14}N , and ^{16}O projectiles. All interactions are of type $n_h=0$. The curve is a Gaussian distribution $\sigma=0.65^\circ$ fitted to the data for $\theta_{\text{proj}} \leq 1.5^\circ$ and corrected for measurement error.

2.1-GeV/nucleon ^{12}C , ^{14}N , and ^{16}O projectiles that are to be compared with the experimental results (Figs. 5 and 6).

Referring to Fig. 5 we find that the narrow, forward peak of $Z=1$ fragments can be fitted by a Gaussian distribution, having a width consistent with the values $\sigma_{Z=1}$ of 1.35–1.45 given in Table

TABLE V. Standard deviation widths of the momentum and projected angular distributions for the $Z=1$ and 2 secondary isotopes from the fragmentation of the CNO group at $E=2.1$ GeV/nucleon. The production-weighted angular widths of $Z=1$ and $Z=2$ fragments are $\sigma_{Z=1}$ and $\sigma_{Z=2}$, respectively. Experimental data are based upon $n_h=0$ type interactions.

| Fragment (wt) | Greiner <i>et al.</i> (Ref. 16) | | Lepore and Riddell (Ref. 30), Eq. (3) | | This experiment exp. (deg) |
|----------------------|---------------------------------|--------------------------------------|---------------------------------------|--------------------------------------|----------------------------|
| | $\sigma(p)$ (MeV/c) | $\sigma(\theta_{\text{proj}})$ (deg) | $\sigma(p)$ (MeV/c) | $\sigma(\theta_{\text{proj}})$ (deg) | |
| p (0.74) | 69 ± 6 | 1.38 ± 0.11 | 79 | 1.58 | |
| d (0.19) | 134 ± 4 | 1.34 ± 0.04 | 107 | 1.07 | |
| t (0.07) | 144 ± 6 | 0.96 ± 0.04 | 126 | 0.84 | |
| | $\sigma_{Z=1} = 1.35 \pm 0.11$ | | | 1.45 | 1.3–1.5 |
| ^3He (0.24) | 150 ± 6 | 1.00 ± 0.04 | 126 | 0.84 | |
| ^4He (0.76) | 130 ± 1 | 0.65 ± 0.005 | 138 | 0.69 | |
| | $\sigma_{Z=2} = 0.73 \pm 0.06$ | | | 0.73 | 0.64 ± 0.02 |

V, provided the large-angle background events can be described by a Gaussian distribution, $\sigma \approx 7.5^\circ$, whose amplitude is about $\frac{1}{3}$ that of the central peak. The large-angle events are primarily pions, although nucleons with high transverse momenta, as suggested by the fireball model,³¹ may be present. Specifically, if we use the temperature and velocity of the projectile fireball estimated by Westfall *et al.*,³¹ i.e., $\beta = 0.91$ and $\tau = 66$ MeV, the width of the momentum distribution, assumed to be Maxwellian, is $\sigma \sim \sqrt{m\tau} = 250$ MeV/ c . The corresponding width of the projected angular distribution for protons is $\sigma(\theta) \sim 7^\circ$, compatible with the 7.5° SD of the observed background. Drawn through the data points in Fig. 5 are curves of the form $N(\theta) = A \exp[-\theta^2/(2\sigma_1^2)] + B \exp[-\theta^2/(2\sigma_2^2)]$, calculated for two values of σ_1 , 1.3° and 1.5° , and $\sigma_2 = 7.5^\circ$. The amplitudes B of the large-angle background distribution illustrated in Fig. 5 are 0.065 and 0.073, and are indicative of the sensitivity of $\sigma_1 \approx \sigma_{Z=1}$ upon background subtraction. Thus, although an accurate estimate of the width of the central peak is not possible, owing to the uncertainty in the spectral shape of the large-angle component, this analysis does lead to the conclusion that the central peak in the $Z=1$ projected angular distribution is due to the hydrogen isotopes produced in the fragmentation of the projectile. The distribution is consistent with being a Gaussian, whose σ width is in satisfactory agreement with the experiments of Greiner *et al.*¹⁶ and the first-order theory of Lepore and Riddell.³⁰

Figure 6 shows the projected angular distribution for the He isotopes from the fragmentation of ${}^{12}\text{C}$, ${}^{14}\text{N}$, and ${}^{16}\text{O}$ nuclei in emulsion projected in the emulsion plane (actually in the x - y plane, where x is along the incident beam track and y is in the plane of the emulsion). Drawn through the distribution is a Gaussian curve whose standard deviation σ is evaluated from data restricted to $\sigma_{\text{proj}} \leq 1.5^\circ$. Correcting the measured widths for measurement error ($\Delta\theta = 0.16 \pm 0.03^\circ$), we obtain $\sigma_{Z=2}(\text{horiz}) = 0.65 \pm 0.02^\circ$. A similar analysis for the vertical phase gives $\sigma_{Z=2}(\text{vert}) = 0.61 \pm 0.05^\circ$, the increase in the error is attributable to the vertical shrinkage of the processed emulsion. Thus, within the errors of this experiment, the transverse momentum distributions for He nuclei projected onto orthogonal planes in the emulsion are equal. The weighted average is $\sigma_{Z=2} = 0.64 \pm 0.02^\circ$.

This measurement of the standard deviation of the projected angular distribution for $Z=2$ fragments appears to be slightly less than that expected from the longitudinal momentum distribution measured by Greiner *et al.* and given by Lepore and Riddell, i.e., $\sigma_{Z=2} = 0.73^\circ$, Table V.

Because the value $\sigma_{Z=2} \approx 0.64^\circ$ was obtained for angles $\theta_{\text{proj}} \leq 1.5^\circ$, hence for angles $\leq 2\sigma_{Z=2}$, the contributions of large, non-Gaussian production angles to the standard deviation are suppressed. Thus the quoted result properly represents a lower limit of $\sigma_{Z=2}$. We therefore argue that the projected angular distributions of hydrogen and helium nuclei produced by the fragmentation of ${}^{12}\text{C}$, ${}^{14}\text{N}$, and ${}^{16}\text{O}$ projectiles at 2.1 GeV/nucleon observed in this experiment are in agreement with those expected from the p distributions measured by Greiner *et al.*, and that to about a 10% level, the momentum distributions of $Z=1$ and $Z=2$ nuclei in the projectile frame are consistent with isotropy.

The principal conclusion we come to, then, is that the projected angular distributions for both $Z=1$ and $Z=2$ fragments emitted from $n_h=0$ type events in emulsion are in agreement with the single-particle inclusive spectra.¹⁶ Thus when we compare the momentum distributions of fragments measured in single-particle inclusive experiments—fragments that are selected only on the basis of their high rapidity (without knowledge of the low-rapidity region)—with the momentum distributions of fragments produced in interactions selected on the basis of the presence of high-rapidity fragments and knowledge of the state of the target-rapidity region, we find no difference between them. This result is a characteristic feature of the hypothesis of limiting fragmentation.

The general features of the angular distribution for $Z=1$ and $Z=2$ secondaries that are portrayed in Figs. 4–6 have been well documented in cosmic-ray heavy-ion experiments. The low intensity of heavy nuclei in the cosmic rays has limited these experiments to studies of the nucleus-nucleus interaction averaged over all impact parameters and energy. Pertinent to this discussion is the work of Andersson *et al.*,³ who examined the angular distribution of shower particles, i.e., high-energy $Z=1$ particles produced in nucleus-nucleus collisions in emulsions by cosmic-ray heavy ions, $3 \leq Z \leq 26$, $E \geq 1.7$ GeV/nucleon, as a function of n_h . They found that as n_h increased from the interval $2 \leq n_h \leq 6$ to $n_h \geq 20$, the probability for a $Z=1$ fragment from the incident projectile to appear within the “proton” peak ($\theta \leq 2.2^\circ$) decreased from 0.40 ± 0.08 to approximately zero (no signal above background). To compare this result with the ($n_h=0$) events examined in this experiment, we find that 0.40 ± 0.02 of the $Z=1$ particles from CNO projectiles are within $\theta_{\text{proj}} \leq 2.0^\circ$. Thus the amplitude of the $Z=1$ fragments produced within $\sim 2^\circ$ of the direction of the incident heavy ions does not depend critically on the n_h for $n_h \leq 6$. The results of Andersson *et al.*, therefore, allow us to extend

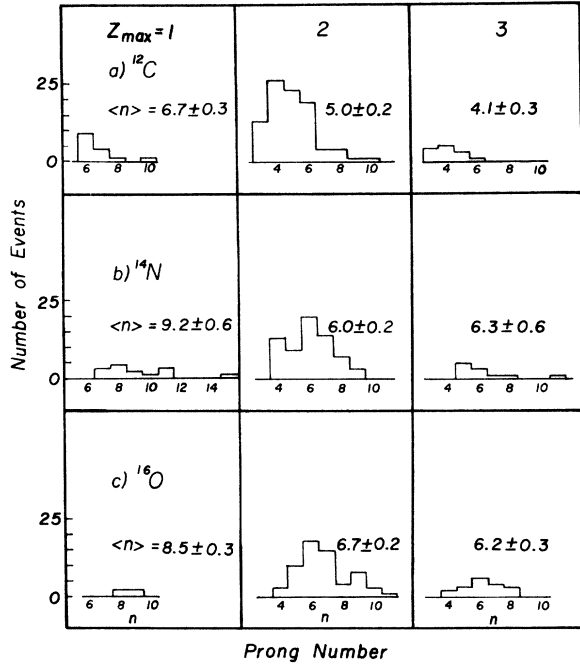


FIG. 7. Histograms of the prong-number distributions for the fragmentation of (a) ^{12}C , (b) ^{14}N , and (c) ^{16}O nuclei in nuclear emulsion, $n_h = 0$ type interactions. Data are ordered as to the maximum charge, Z_{\max} , emitted in the fragmentation for $1 \leq Z_{\max} \leq 3$ only. The mean prong number $\langle n \rangle$ is indicated for each distribution.

the application of the concept of limiting fragmentation to target-projectile interactions that exhibit a small but finite number of target prongs in the low-rapidity region. Thus there is evidence that projectile fragmentation distributions remain uncorrelated with target fragmentation for $n_h \leq 6$.

C. Prong-number and prong-multiplicity distributions

To demonstrate some of the topological features of the fragmentation process for the $n_h = 0$ type interactions, we plot in Fig. 7 the charged-prong number (n), and in Fig. 8 the charge-multiplicity (Z^*) distributions of the secondary fragments as a function of Z_{\max} , the charge of the principal fragment, i.e., highest Z produced in the fragmentation of ^{12}C , ^{14}N , and ^{16}O projectiles. The quantity $Z^* = \sum_{i=1}^n |Z_i|$ is the sum of the (absolute) charges of the n secondary particles. Table VI presents the production frequency of events also categorized according to Z_{\max} . These data have been corrected for scanning losses for events $Z_{\max} \geq 4$ (Table II). Because of the small number of events observed to have $Z_{\max} \geq 4$ and the cited difficulties in their detection, we shall limit our discussion to fragmentation events that have $1 \leq Z_{\max} \leq 3$ only; events

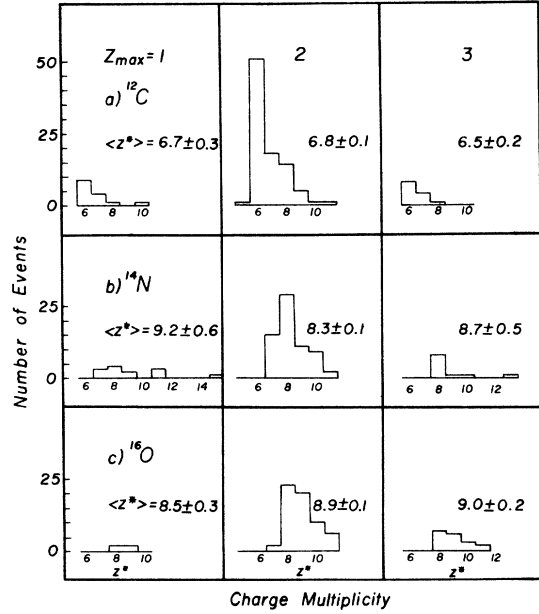


FIG. 8. Histograms of the charge multiplicity distributions for the fragmentation of (a) ^{12}C , (b) ^{14}N , and (c) ^{16}O . The quantity $Z^* = \sum_{i=1}^n |Z_i|$, where $|Z_i|$ is the absolute charge of the n th prong. The histograms are based upon the same events used for Fig. 7, and are also ordered as to Z_{\max} . The mean-charge multiplicity is indicated for each distribution.

for which scanning losses are negligible.

Before discussing some of the details presented in Figs. 7 and 8, we wish to point out that in no case, out of 1000 observed interactions for each of the ^{12}C , ^{14}N , and ^{16}O beam projectiles, did we observe a fragmentation event that yielded two or more secondaries with $Z > 2$, irrespective of the amount of target excitation. Thus two-product fragmentation events such as $^{14}\text{N} \rightarrow ^7\text{Be} + ^7\text{Li}$ were not observed. The cross section for their production is therefore $\leq 10^{-3}$ of the total reaction cross section.

Notable features of the data presented in Figs. 7 and 8 are the following:

- (i) For $Z_{\max} = 1$ events (where all fragments are

TABLE VI. Production frequency, in percent, of events in emulsion as a function of Z_{\max} , the highest charged projectile fragment produced in interaction. Corrections for scanning losses for events for $Z_{\max} \geq 4$ are included.

| Projectile | Z_{\max} | | | |
|-----------------|------------|-------------|-----------|-------------|
| | 1 | 2 | 3 | ≥ 4 |
| ^{12}C | 7 ± 2 | 59 ± 10 | 8 ± 3 | 26 ± 12 |
| ^{14}N | 11 ± 4 | 49 ± 13 | 8 ± 3 | 32 ± 17 |
| ^{16}O | 2 ± 1 | 33 ± 5 | 9 ± 2 | 55 ± 6 |

singly charged, hence, include only the hydrogen isotopes and mesons of both charges) the number of prongs (Fig. 7) are in all cases equal to, or greater than, the atomic number of the projectile. The largest number of prongs detected in this sample is a ${}^{14}\text{N}$, $Z_{\text{max}}=1$ fragmentation that has 15 minimally ionizing secondaries. The excess of eight charged particles, if we assume seven of the charges are due to hydrogen isotopes from the ${}^{14}\text{N}$ projectile, implies that multiple-pion production can occur in nucleus-nucleus collisions, even though the target nucleus (if it is not hydrogen) does not receive sufficient excitation energy to emit particles.

(ii) Fragmentations in which $Z_{\text{max}}=2$, i.e., no fragments with charge $Z > 2$, is a highly probable configuration for all projectiles. The ${}^{12}\text{C} \rightarrow 3\alpha$ reaction is the only contributor to the three-prong $Z_{\text{max}}=2$ events for carbon, as is the ${}^{14}\text{N} \rightarrow 3\text{He} + \text{H}$ reaction to the four-prong events in nitrogen, each comprising about 10% of their respective $n_h=0$ events. The four- α breakup of ${}^{16}\text{O}$ is considerably less probable than the ${}^{12}\text{C} \rightarrow 3\alpha$ reaction, occurring in only about 1% of the $n_h=0$ ${}^{16}\text{O}$ events. We note also that complete breakup into $Z=1$ fragments is less probable for ${}^{16}\text{O}$ than it is for ${}^{12}\text{C}$ and ${}^{14}\text{N}$.

(iii) The topologies of ${}^{12}\text{C}$ and ${}^{16}\text{O}$ fragmentations are the same—the differences between them are attributable primarily to the differences in the masses of these projectiles. The $\langle n \rangle$ values for ${}^{12}\text{C}$ and ${}^{16}\text{O}$ show the same trends for each Z_{max} ; for example, within the errors of the data, $\langle n \rangle({}^{16}\text{O}) \approx \langle n \rangle({}^{12}\text{C}) + 2$. Also, the excess of charge $Z^* - Z_B$ observed in the fragmentation products of ${}^{12}\text{C}$ (0.7 ± 0.1) and ${}^{16}\text{O}$ (0.9 ± 0.1) is approximately 10% of the charge of the incident ion.

(iv) Three events were observed in which the net charge emitted from the interaction (${}^{12}\text{C}$ and ${}^{16}\text{O}$) is one unit of charge less than the charge of projectile. Although undetected singly-charged tracks could account for them, the number of such events can be accounted for by charge-exchange ($p \rightarrow n$) reactions between the projectile and target nucleons, provided the cross section is the order of $100 \mu\text{b}$.

(v) The fragmentation of ${}^{14}\text{N}$ nuclei shows differences when compared with the ${}^{12}\text{C}$ and ${}^{16}\text{O}$ data: These are the high probability for complete fragmentation of ${}^{14}\text{N}$ into $Z=1$ particles ($11 \pm 4\%$ versus $7 \pm 2\%$ and $2 \pm 2\%$ for ${}^{12}\text{C}$ and ${}^{16}\text{O}$, respectively) and the high multiplicity of these events, 9.2 ± 0.6 . The $\langle Z^* \rangle$ for ${}^{14}\text{N}$ is $8.5 \pm 0.1_4$ for the $1 \leq Z_{\text{max}} \leq 3$ events, giving a charge excess of 1.5 ± 0.1 —about twice that observed for ${}^{12}\text{C}$ and ${}^{16}\text{O}$. The elimination of the two highest values of $Z^* = 13$ and 15 from the ${}^{14}\text{N}$ spectrum reduces the charges excess to 1.3 ± 0.1 , illustrating that this quantity is not signifi-

cantly influenced by the tail of the ${}^{14}\text{N}$ Z^* distribution.

(vi) Whereas the modes of the Z^* histograms, Fig. 8, for ${}^{12}\text{C}$ and ${}^{16}\text{O}$ occur at $Z^* = Z_B$, the atomic number of the incident ion, the mode of the Z^* distribution for incident ${}^{14}\text{N}$ is $Z_B + 1$.

That the most probable value for Z^* for ${}^{14}\text{N}$ fragmentation is $Z^* = 8$ may be statistical in nature, particularly because of the small number of events. It leads, however, to the question of whether there was ${}^{16}\text{O}$ contamination of the ${}^{14}\text{N}$ beam. From an analysis of the interactions and beam tracks themselves in the emulsion, we found no direct, or indirect, evidence for beam impurities in the ${}^{14}\text{N}$ data. For example, the fragmentation of ${}^{16}\text{O} \rightarrow 4\text{He}$ (with or without accompanying shower particles) is a reaction unique to ${}^{16}\text{O}$, and its detection in the ${}^{14}\text{N}$ data would unequivocally indicate the presence of ${}^{16}\text{O}$. No such event was observed in this experiment, nor in the study of a comparable number of ${}^{14}\text{N}$ interactions by Judek,³² who has analyzed several plates from our emulsion stack, as well as emulsions exposed to the same ${}^{14}\text{N}$ beam. Specifically, no 4He events were observed in a sample of 91 ${}^{14}\text{N}$ interactions for which $Z = 2$ and $n_h = 0$. Based on the ${}^{16}\text{O}$ data from this experiment and Ref. 22, the probability for the reaction ${}^{16}\text{O} \rightarrow 4\text{He}$ (for the type $Z_{\text{max}}=2$, $n_h=0$) is $\sim 9\%$, i.e., 7 events in 81 interactions. Given this probability, we would expect a 50% chance of observing at least one 4He event in the ${}^{14}\text{N}$ data had there existed a 12% ${}^{16}\text{O}$ background in the ${}^{14}\text{N}$ beam. If we take 12% as an upper limit to the ${}^{16}\text{O}$ background, a maximum of eight ${}^{16}\text{O}$ events could contribute to the Z^* histogram for ${}^{14}\text{N}$ (Fig. 8). If we assume that the Z^* values of these events would be distributed the same as those observed for ${}^{16}\text{O}$, then the corrections to the ${}^{14}\text{N}$ data would be less than the statistical errors at all values of Z^* . Thus an upper limit of ${}^{16}\text{O}$ background events, derived statistically from the lack of 4He events in the ${}^{14}\text{N}$ data, could not, if present, alter significantly the Z^* distributions for ${}^{14}\text{N}$ as observed.

If we choose to consider the differences between the fragmentation topologies of ${}^{14}\text{N}$ relative to ${}^{12}\text{C}$ and ${}^{16}\text{O}$ as real, then they must be a manifestation of the differences in the nuclear structure of the projectile nuclei. As an example, ${}^{14}\text{N}$ is an odd-odd, $I=1$ nucleus, while ${}^{12}\text{C}$ and ${}^{16}\text{O}$ are both even-even (α particle) nuclei with $I=0$. In evidence, therefore, is that nuclear structure of the projectile may play an important role in the fragmentation process. This observation complements the results of Greiner *et al.*¹⁶ and Lindstrom *et al.*¹³ where effects attributable to the structure of fragment nuclei are apparent in the systematics of the longitudinal momentum distributions and isotope

production cross sections. Of particular interest is the indication that ^{14}N produces, on the average, a net charge excess per fragmentation that is about $0.7 e$ greater than that observed for ^{12}C and ^{16}O . Because this increase in charge multiplicity is most likely due to pions, an implication is that the pion-production cross section by 2.1-GeV/ n ^{14}N is greater than those by ^{12}C and ^{16}O on nuclei for the particular class of fragmentation reactions we have examined, i.e., those with no visible target fragmentation. Whether or not this possible enhancement of pion production by ^{14}N is limited to peripheral collisions, where nuclear structure effects become important, can only be conjectured at this time. The revelation of any impact-parameter dependence (e.g., as indicated by the number of evaporation and knock-on fragments from target nuclei) on pion-production cross sections in heavy-ion collisions necessarily requires further experimentation.

IV. SUMMARY

In this comparative study on the interactions of relativistic nuclei in nuclear research emulsion we have measured the mean-free-path lengths of ^4He , ^{12}C , ^{14}N , and ^{16}O nuclei at 2.1 GeV/nucleon, and have examined the topological features of the projectile fragmentation of ^{12}C , ^{14}N , and ^{16}O nuclei, with specific attention to the angular distributions of the $Z=1$ and 2 fragments and the prong and charge-multiplicity distributions.

By fitting the mean-free-path data to Karol's soft-spheres (optical) model,²⁸ we are able to determine the effective, mean nucleon-nucleon cross section $\bar{\sigma}$ that accounts for the experimental observations. Our finding is that the effective nucleon-nucleon cross section is $0.52 \pm 0.06 (=K)$ of the average, free nucleon-nucleon cross section at 2.1 GeV. Our conclusion, therefore, is that the mean-free-path measurements in emulsion do not constitute a measure of the total reaction cross section (one which corresponds to $K \approx 1$), but determine a cross section that involves greater inelasticity and increased energy transfer more properly identified with nucleus transmutation reactions.

We have pointed out that the optical model calculations of Karol²⁸ and Barshay *et al.*²⁷ can be ordered in terms of A_{min} , the smaller mass number of the interacting nuclei, to exhibit the traditional form of the Bradt-Peters relation (Fig. 1). The dependences of the parameters r_0 and b on A_{min} , appropriate for $K=0.52$, are illustrated in Fig. 2. Whereas r_0 is quite insensitive to A_{min} , the overlap parameter b decreases monotonically

with A_{min} to an $A_{\text{min}} \approx 30$, becoming approximately constant thereafter. Such behavior is consistent with the diminution of nuclear transparency with increasing mass of the interacting nuclei.

The projected angular distributions for $Z=1$ (corrected for background of large P_{\perp} fragments) and $Z=2$ fragments emitted from $n_h=0$ type events in emulsion are found to be in agreement with those expected from the longitudinal momentum distributions observed in single-particle inclusive experiments. The angular distribution data thus indicate that the momentum distributions are consistent with isotropy in the projectile frame, and serve to demonstrate the validity of the limiting fragmentation process when heavy-ion interactions are selected on the basis that the states are specified in both the high- and low-rapidity regions.

We concluded this experiment with an exposition of the prong and charge-multiplicity distributions of high-rapidity (projectile) fragments produced in $n_h=0$ type events. The notable feature of these data is the observation that the (absolute) charge multiplicities are, on the average, about 10% greater than the charge of the incident nucleus. That the charge-excess produced in ^{14}N interactions is greater than that produced by either ^{12}C or ^{16}O projectiles is suggested by the data. Complementing this result is the observation that $n_h=0$ type events with the largest charge excess occurred in the fragmentation of ^{14}N projectiles, where Z^* 's up to 13 and 15, all high-velocity, $Z=1$ particles were detected—suggesting that significant pion production can take place, albeit with very low target excitation.

ACKNOWLEDGMENTS

The authors wish to thank the Bevatron staff and operating crew under Robert Force, Hermann Grunder, and Walter Hartsough for their assistance and support in carrying out this experiment. Our scanning and measuring technicians, Ridgway Banks, Margaret Bassett, Ernestine Beleal, Dennis Jones, Gary Williams, and Robert Smith, who also processed the nuclear emulsions, are commended for their careful and exacting work. We also appreciate our informative discussions with Dr. T. F. Hoang and Dr. B. Judek. We especially appreciate Dr. Judek's willingness to make available to us her experimental results before publication. This work was performed under the auspices of the U. S. Energy Research and Development Administration under Contract No. W-7405-ENG-48 and the National Aeronautics and Space Administration under Grant No. NGR-05-003-513.

- ¹P. Frier, E. J. Lofgren, E. P. Ney, F. Oppenheimer, H. L. Brandt, and B. Peters, *Phys. Rev.* **74**, 213 (1948).
- ²C. J. Waddington, *Prog. Nucl. Phys.* **8**, 1 (1960).
- ³B. Andersson, I. Otterlund, and K. Kristiansson, *Ark. Fys.* **31**, 527 (1966).
- ⁴I. Otterlund, *Ark. Fys.* **38**, 467 (1968).
- ⁵R. Kullberg and I. Otterlund, *Z. Phys.* **259**, 245 (1973).
- ⁶I. Otterlund and B. Andersson, *Ark. Fys.* **35**, 133 (1967).
- ⁷R. Kullberg, I. Otterlund, and R. Resman, *Phys. Scr.* **5**, 5 (1972).
- ⁸R. Resman and I. Otterlund, *Phys. Scr.* **4**, 183 (1971).
- ⁹I. Otterlund and R. Resman, *Ark. Fys.* **39**, 265 (1969).
- ¹⁰W. R. Frazer, L. Ingber, C. H. Mehta, C. H. Poon, D. Silverman, K. Stowe, P. D. Ting, and H. J. Yesian, *Rev. Mod. Phys.* **44**, 284 (1972).
- ¹¹H. H. Heckman, D. E. Greiner, P. J. Lindstrom, and F. S. Bieser, *Phys. Rev. Lett.* **28**, 926 (1972).
- ¹²H. H. Heckman, in *Proceedings of the Fifth International Conference on High Energy Physics and Nuclear Structure, Upsala, Sweden, 1973*, edited by G. Tibbell (Elsevier, New York, 1974).
- ¹³P. J. Lindstrom, D. E. Greiner, H. H. Heckman, Bruce Cork, and F. S. Bieser, Lawrence Berkeley Laboratory Report No. LBL-3650, 1975 (unpublished).
- ¹⁴G. M. Raisbeck and F. Yiou, *Phys. Rev. Lett.* **35**, 155 (1975).
- ¹⁵H. H. Heckman and P. J. Lindstrom, *Phys. Rev. Lett.* **37**, 56 (1976).
- ¹⁶D. E. Greiner, P. J. Lindstrom, H. H. Heckman, B. Cork, and F. S. Bieser, *Phys. Rev. Lett.* **35**, 152 (1975).
- ¹⁷P. J. Lindstrom, D. E. Greiner, and H. H. Heckman, *Bull. Am. Phys. Soc.* **17**, 488 (1972); also H. H. Heckman, *Relativistic Heavy Ion Seminar, Internal LBL Report, 1973* (unpublished).
- ¹⁸P. J. Lindstrom, D. E. Greiner, H. H. Heckman, B. Cork, and F. S. Bieser, in *Proceedings of the Fourteenth International Conference on Cosmic Rays, Munich, 1975*, edited by Klaus Pinkau (Max-Planck-Institute, München, 1975), Vol. **7**, 2315.
- ¹⁹T. F. Cleghorn, Ph.D. thesis, University of Minnesota, 1967 (unpublished).
- ²⁰C. J. Waddington, *Prog. Nucl. Phys.* **8**, 1 (1960).
- ²¹B. Jakobsson, R. Kullberg, and I. Otterlund, in *Proceedings of the Fourteenth International Conference on Cosmic Rays, Munich, 1975*, edited by Klaus Pinkau (Max-Planck-Institute, München, 1975), Vol. **7**, p. 2353.
- ²²B. Judek, in *Proceedings of the Fourteenth International Conference on Cosmic Rays, Munich, 1975*, edited by Klaus Pinkau (Max-Planck-Institute, München, 1975), Vol. **7**, p. 2342.
- ²³E. Lohrmann and M. W. Teucher, *Phys. Rev.* **115**, 636 (1959).
- ²⁴H. C. Bradt and B. Peters, *Phys. Rev.* **77**, 54 (1950).
- ²⁵D. L. Cheshire, R. W. Huggett, D. P. Johnson, W. V. Jones, S. P. Rountree, S. D. Verma, W. K. H. Schmidt, R. J. Kurz, T. Bowen, and E. P. Krider, *Phys. Rev. D* **10**, 25 (1974).
- ²⁶W. H. Barkas, *Nuclear Research Emulsions* (Academic, New York, 1963), Vol. **1**.
- ²⁷S. Barshay, C. B. Dover, and J. P. Vary, *Phys. Rev. C* **11**, 360 (1975); also J. P. Vary (private communication).
- ²⁸P. J. Karol, *Phys. Rev. C* **11**, 1203 (1975).
- ²⁹J. P. Vary, private communication.
- ³⁰J. V. Lepore and R. J. Riddell, Jr., Lawrence Berkeley Laboratory Report No. LBL-3086, 1974 (unpublished).
- ³¹G. D. Westfall, J. Gosset, P. J. Johansen, A. M. Poskanzer, W. G. Meyer, H. H. Gutbrod, A. Sandoval, and R. Stock, *Phys. Rev. Lett.* **37**, 1202 (1976).
- ³²B. Judek, private communication.

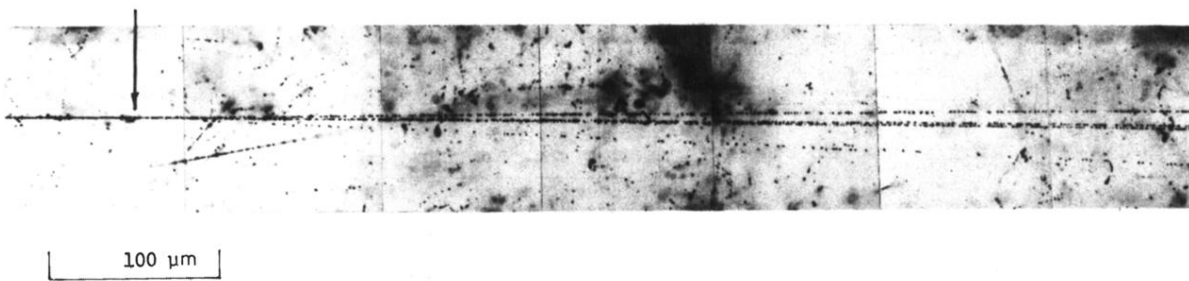


FIG. 3. Photomicrograph of the fragmentation of a 2.1-GeV/N ^{14}N nucleus in nuclear emulsion. The point of interaction is indicated by the arrow. The ^{14}N enters from the left, fragments into 3He + H, with no emission of low-energy, heavily ionizing tracks.